

www.wcee2024.it

# PERFORMANCE OF A 10-STORY STEEL STAIR TOWER WITHIN THE NHERI TALLWOOD BUILDING

S. Sorosh<sup>1</sup>, T.C. Hutchinson<sup>1</sup>, K. L. Ryan<sup>2</sup>, K. Smith<sup>3</sup>, R. Belvin<sup>3</sup>, A. Kovac<sup>3</sup>, S. Pei<sup>4</sup> & D.M. Dowden<sup>5</sup>

<sup>1</sup> Department of Structural Eng., University of California San Diego, CA, USA,

ssorosh@ucsd.edu; tara@ucsd.edu

<sup>2</sup> Department of Civil and Environmental Eng., University of Nevada Reno, USA
<sup>3</sup> Construction Specialties, PA, USA

<sup>4</sup> Department of Civil and Environmental Eng., Colorado School of Mines, CO, USA

<sup>5</sup> Department of Civil, Environmental, and Geospatial Eng., Michigan Technological University, MI, USA

Abstract: Stairs provide the primary egress in and out of a building during and after an earthquake event. Previous earthquake events and experimental studies revealed that stairs with fixed connections at multiple levels within a building result in damage to both the stair system and its supporting structure. Catastrophic failure of stairs has been reported during recent events, most notably during the 2011 Christchurch earthquake and the 2023 Kahramanmaras earthquake sequence. Therefore, understanding the seismic response of these drift-sensitive non-structural systems is essential. Moreover, stair systems are exposed to multi-support excitations induced by floor accelerations and interstory drifts. To mitigate damage to stair systems and the supporting structure, resilient stair connections with a variety of detailing options have been proposed. Notable options include stairs with fixed-free connections, sliding-slotted connections, and drift-compatible detailing. A unique system-level experimental study adopting the aforementioned resilient detailing concepts is conducted on the tallest ever 10-story prefabricated steel stair tower integrated within the NHERI TallWood mass timber building test program at the UC San Diego 6-DOF Large High-Performance Outdoor Shake Table (LHPOST6). This paper will present preliminary findings and results from this shake table test program.

# 1. Introduction

Stair systems, spanning vertically across multiple floors and subject to interstory drift induced by seismic activity, are characterized as displacement-sensitive non-structural systems. Previous earthquake events consistently documented the extensive and catastrophic damage incurred by these essential non-structural systems. Notably, Li and Mosalam (2013) reported significant damage experienced by concrete stairs during the 2008 Wenchuan earthquake. Subsequently, Bull (2011) provided a comprehensive summary of the damage sustained by both concrete and steel stairs in the aftermath of the 2011 Christchurch earthquake. Recently, substantial damage to stair systems have been reported during the 2023 Kahramanmaras earthquake sequence in Turkey (Dilsiz et al., 2023, Altunsu et al. 2024).

Previous experimental studies have demonstrated that the overall behavior of the stair system is significantly influenced by the flexibility of its connections. Notably, Higgins (2009) conducted an experiment to study the response of steel stairs under reversed cyclic quasi-static loading. Although, during their tests, a design target peak interstory drift ratio of 2.5% was achieved, significant local deformations at the stair flight to landing connection were observed. Subsequently, as part of the shaking table test of a full-scale five-story reinforced concrete building, an operable prefabricated steel stair was studied by Hutchinson et al. (2013) at UC San Diego. These shake table tests reported fracture in the stair connections and slab-embedded welds prior to reaching the design-targeted peak interstory drift ratio (PIDR) of 2.0-2.5% (Wang et al., 2013, 2015; Pantoli et al., 2013).

Based on the generally poor performance of stair systems observed in the aftermath of previous seismic events and experimental investigations, it has been concluded that stair systems incorporating fixed flight-to-landing connections are highly vulnerable to complete loss of functionality. As a result, ASCE 7-16 (2017), Section 13.5.10 mandates that egress stairs, when not part of the seismic force-resisting system, must be designed to accommodate relative displacements between two levels without compromising their stability or function of gravity support. In line with this requirement, two extensive shake table testing programs were conducted at the University of Nevada, Reno Earthquake Engineering Laboratory, focusing on full-scale prefabricated steel stair assemblies featuring a variety of drift-compatible connection configurations (Black et al., 2017, 2020). These testing programs employed several connection strategies, including a fixed connection at the top and a free-sliding connection at the bottom (fixed-free configuration), longitudinal slots at the top and transverse slots at the base (slotted connection), and an industry-designed drift-compatible connection at the top with a fixed connection at the base (fixed-drift compatible configuration). Among these configurations, the stair system with a fixed-drift compatible configuration exhibited excellent performance and remained undamaged when subjected to a target MCE-scaled earthquake. However, stair systems with fixed-free configurations sustained significant damage when exposed to MCE-level earthquakes. Stairs with slotted connections performed well under earthquakes with smaller amplitudes but experienced binding at the connections during earthquake tests with larger amplitudes.

To further study the seismic response of stair systems with various resilient (drift release, or targeted damage-free) connection detailing, system level tests with realistic boundary conditions are needed. A 10-story steel stair tower was tested as part of the NHERI TallWood 10-story mass timber building at the UC San Diego 6-DOF Large High-performance Outdoor Shake Table (LHPOST6). This paper provides a brief overview of the test program with a focus on the performance of the 10-story stair systems installed in the building specimen. Pei et al. (2023) discuss an overview of the testing program and building response in more detail.

# 2. Shake table test program

The increasing popularity of mass timber construction stems from its eco-friendly features, lower carbon footprint, and potential to expedite construction compared to traditional materials like concrete and steel. Nevertheless, it remains crucial to prioritize proper design, construction, and maintenance practices to ensure the long-term resilience and safety of mass timber structures. Therefore, to advance the use of a new seismic resilient lateral system using post-tensioned (PT) mass timber rocking walls along with U-shaped flexural plates (UFP) to dissipate energy, a series of shake table tests were conducted on a 10-story mass timber building at the UC San Diego 6-DOF Large High-Performance Outdoor Shake Table (LHPOST6). In addition, subsequently, the response of an innovative uplift friction-based damper was studied as a payload phase of this shaking table test program.

Integrated within this building specimen was a full-scale 10-story stair tower assembled with a variety of drift-release connections intended to minimize drift-induced damage and preserve full functionality of the sole egress/ingress to the building. This section provides a brief overview of the TallWood building test specimen, the friction-based damper payload tests, the design details of the stair systems, and the test protocol.

# 2.1. TallWood building specimen

The TallWood project features a 10-story mass timber building, attached to the large high-performance 6-DOF outdoor shake table (LHPOST6) at UC San Diego, with a height of 112 feet, see Figure 1a. The test building was designed with three distinct floor plans, incorporating a blend of commercial, office, and residential occupancies. The primary objective of the NHERI TallWood project is to propel the adoption of an innovative

seismic-resistant lateral system, which employs post-tensioned (PT) mass timber rocking walls alongside U-shaped flexural plates (UFP) to effectively dissipate energy. As seen in Figure 1, two mass timber rocking walls function as the lateral resisting system along each perpendicular axis of the building. In the east-west direction, the primary lateral system is comprised of cross-laminated timber (CLT) rocking walls, while in the north-south direction, two mass plywood panel (MPP) rocking walls serve as the lateral system. Diverse mass timber components, including CLT, glue-laminated timber (GLT), nail-laminated timber (NLT), and dowel-laminated timber (DLT), are utilized for the floor diaphragms. Serving as the central focus of the NHERI TallWood multidisciplinary industry-university research program, the 10-story mass timber building symbolizes the culmination of these efforts. For more details on the design of the structural system refer to Busch (2023), Huang (2023), Wichman (2023), and Pei et al. (2023).

Vertically distributed non-structural systems were also incorporated into the TallWood building. Notably, a full-scale operable 10-story stair tower, as well as exterior and interior cold-formed steel (CFS) wall subassemblies, and a two-story fire-rated curtain wall subassembly were incorporated, each detailed to accommodate drift. Each exterior and interior cold-formed steel wall and the curtain wall subassembly featured a variety of drift-compatible connections, including expansion joints, double slip track joints, and slotted slip track joints. Additional information regarding the design and the response of the non-structural wall subassemblies may be found in Roser et al. (2022) and Wynn et al. (2022).

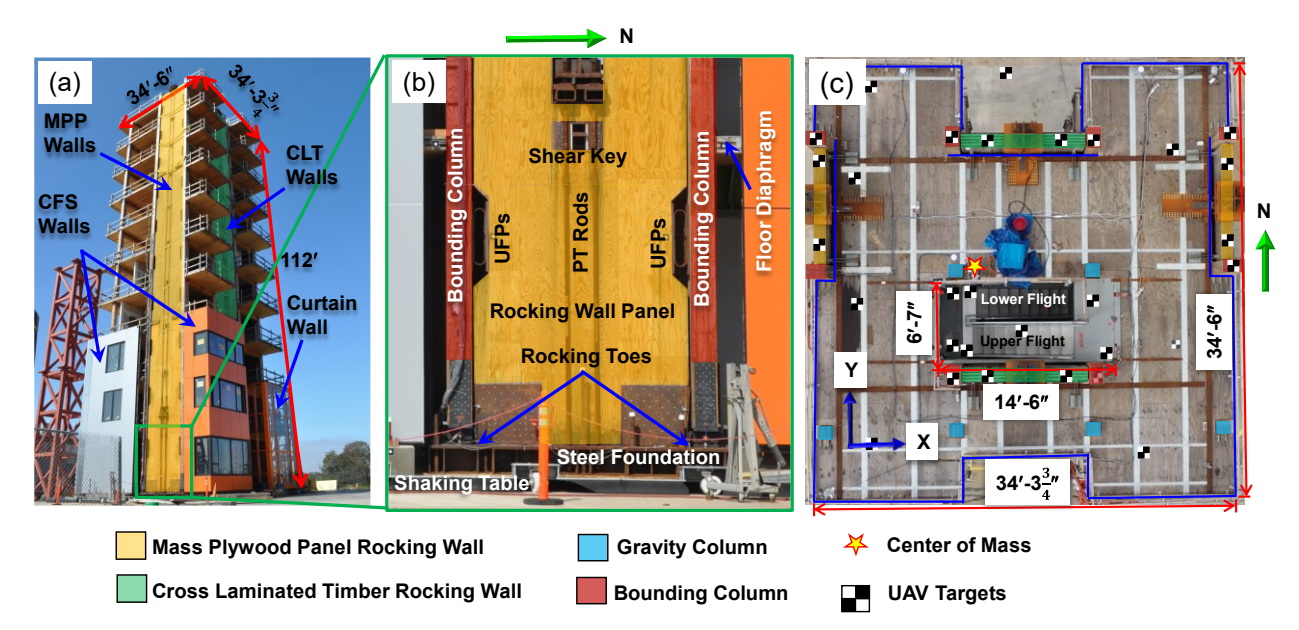


Figure 1: 10-story NHERI TallWood building specimen: (a) isometric view of complete as-built specimen, (b)

Elevation view of rocking wall subassembly, and (c) floor plan view at the roof

# 2.2. Uplift friction-based damper payload testing specimen

The objective of the payload tests mentioned earlier was to validate the performance of a proposed Uplift Friction Damper (UFD) for mass timber rocking walls that provides alternative energy dissipation, enhanced self-centering capabilities and simplified repair/replacement needs post-earthquake. A detailed presentation describing the kinematics of the UFD is presented in Tatar and Dowden (2022). The UFDs were installed as added supplemental energy dissipation elements, while all other existing conditions of the test building remain unchanged. Furthermore, the UFDs were installed on walls in only one primary direction. Since the UFDs were installed after the NHERI TallWood testing was finished, the MPP walls in the N-S direction were selected to avoid interference with the building's central stair core (see Figure 2). These additional shake table tests validated the seismic performance of the UFDs subjected to real simulated earthquakes on a test building with realistic boundary conditions and preliminary results presented in Dowden and Tatar (2024). Furthermore, these additional shake table tests provided additional data to characterize the seismic performance of the central stair core with emphasis on the weak axis of the stair system.

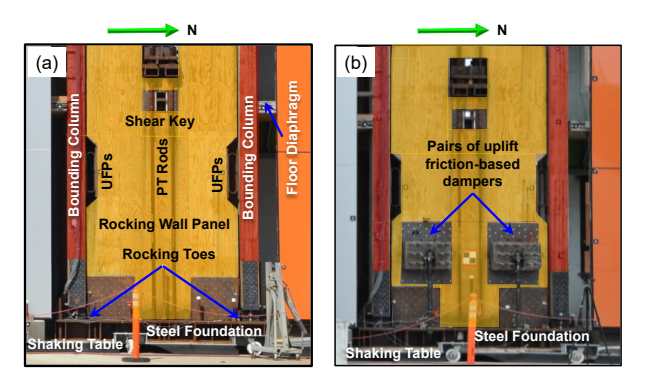


Figure 2: East MPP rocking wall base configuration: (a) original phase-1, and (b) payload configuration

### 2.3. Design details of the 10-story stair tower

A 10-story prefabricated steel scissor-style stair tower was erected within the central region of the building specimen adjacent to the south CLT wall (see Figure 1c) resulting in a diaphragm opening of 6.5 ft by 14.5 ft. The footprint of the building covers an area of 34.5 ft by 34.25 ft area at its edges. In this configuration, the stair system is placed such that its strong axis aligns with the east-west (X) axis of the building, while the transverse or weak axis of the stair system runs along the north-south (Y) axis of the building.

The stair tower incorporated in this building specimen consists of eight stories utilizing a unique story-level complete modular unit (Modular Stair System, MSS) with gravity columns spanning from floor to floor and the upper two stories (9 and 10) were assembled according to traditional (stick-framed) construction that lacks the floor-to-floor gravity columns. The MSSs are self-supporting modules that were prefabricated off-site and entirely preassembled off of the building and installed as a single story, stacking each story to create the complete tower. Such a system is appealing as it allows for shop-level control of construction tolerances and reduction of on-site construction time and often eliminates the need for scaffolding or temporary stair systems during construction until such time that traditional stair systems are installed. Traditional construction methods for stair systems, on the other hand, involve the assembly of individual components (stair flights, handrails, landings, gravity columns) on-site during building construction.

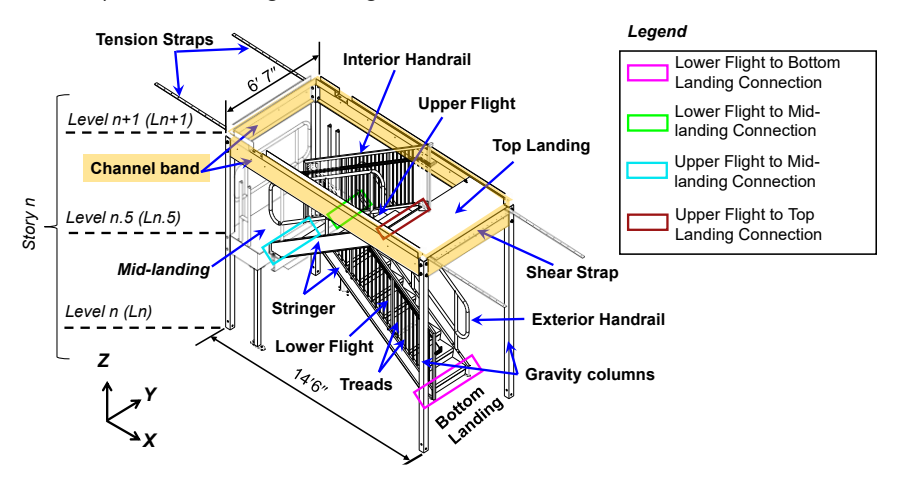


Figure 3: Three-dimensional schematic of a single story of the modular scissor-style stair with key components annotated

Typically, stair systems are designed with stair flights directly connected to the floor diaphragm. However, in this test program, each stair story incorporates landings and a complete channel band as shown in Figure 3. The stair channel band attaches to the floor diaphragm using four tension straps and two shear straps or steel angles at each level (Figure 3). The design details of these connections are elaborated in Sorosh et al. (2022a,b). Stair systems, attached at multiple levels within a building, are exposed to multi-support excitation due to floor movements. The relative displacement between subsequent floor levels, known as interstory drift, places stress on stair connections, potentially resulting in stair system and/or structural system damage or failure. The concept underlying the design of the stair tower in the TallWood building was to minimize such

damage anticipated during rocking-induced interstory drift demands imposed during the extensive earthquake sequence imposed on the building.

The interstory drifts were accommodated through flexible and drift-compatible connections between the stair flight and landings. A variety of connection details including drift-compatible, slotted, and free types of connections were considered in this test program. Figure 4 shows a rendering of the stair tower with the specific connection details implemented. The seismic response of the stair system, especially the connection response, at stories 2,3,4,6,8, and 10 were recorded using a dense array of accelerometers, linear potentiometers, string potentiometers, and strain gauges. In total 109 analog sensors and 14 high-resolution video cameras were used to monitor the stair system response.

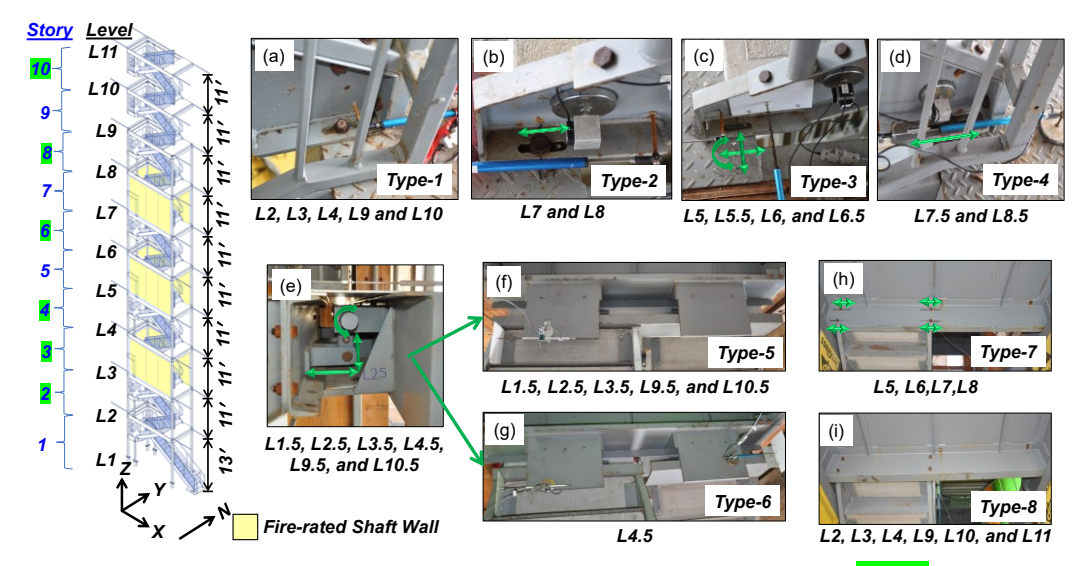


Figure 4: Stair tower connection details (instrumented stories highlighted in green): (a) longitudinal (construction) slotted connection, (b) longitudinal (short) slotted connection with snug tightened bolt, (c) free (resting) connection, (d) longitudinal (long) slotted connection with snug tightened bolt, (e) drift-compatible (Drift-Ready<sup>TM</sup>) connection, (f) single attachment channel detail, (g) dual attachment channels, (h) lateral slotted connection with snug tight bolt, and (i) fixed connection

Stories 1 through 4 and stories 9 and 10 featured stair systems with drift-compatible connections (DC) at the mid-landing level, see Figure 4. The drift-compatible connections, offering three degrees of freedom as marked in green arrows in Figure 4e, are detailed such that they provide free movement of the stair flight at the mid-landing level. As illustrated in Figures 4f and 4g, two attachment strategies were employed to connect the stair flight to the drift-compatible connections. Namely, at levels 1.5, 2.5, 3.5, 9.5, and 10.5 a single attachment channel, with both the lower and upper stair flight attached was utilized (Figure 4f). In contrast, at level 4.5, a dual attachment channel, allowing each stair flight to move independently was utilized (Figure 4g). In stories where a drift-compatible connection was implemented at the mid-landing level, the lower flight to bottom landing connection was detailed with a longitudinal slotted connection, consisting of construction slots approximately 1.5 inches in length, as shown in Figure 4a. These slotted connections were specifically designed to accommodate construction tolerances, and the bolts at these connections were securely tightened using an impact hammer. Thus, following construction fit-up, only movement along the slot is anticipated if bolt pre-tension is overcome. In contrast, the upper flight to the top landing connection in these stories (stories 1 through 4 and stories 9 and 10) featured a fixed connection with an insignificant construction tolerance, as depicted in Figure 4i.

In stories 5 and 6, both the lower flight to bottom landing and the upper flight to mid-landing connections are of the free type of connection (FC), where the stair flight rests on the landings without any bolts securing them together (refer to Figure 4c). These connections offer two translation degrees of freedom ( $\Theta_Z$ ) and one rotational degree of freedom ( $\Theta_Z$ ). The lower flight to the mid-landing connections at these two stories are of the 'fixed' type. Furthermore, the upper flight is attached to the top-landing channel using transverse slotted connections (Figure 4h).

In stories 7 and 8, the longitudinal slotted connections (SC) with one degree of freedom ( $\Delta x$ ) were featured at the bottom connections of each flight. The slotted holes at the lower flight to the bottom landing connections (Figure 3b) are shorter than those at the upper flight to mid-landing connections (Figure 3d). The lower-flight to mid-landing connections were fixed. Transverse slotted connections were utilized at the upper flight to the top landing (Figure 4h). It is worth noting that the bolts at the slotted connections were "snug tightened" to allow movement, unlike fixed connections and the construction slotted connections that were tightened using an impact hammer.

#### 2.4. Test protocol

On May 1, 2023, Phase 1 of shaking table tests commenced and lasted for a duration of 3 weeks, concluding on May 22. During Phase 1, the building underwent testing with a total of 88 ground motions, followed by an additional 10 ground motions during the payload tests. The suites of ground motions used in this shaking table test program were selected for site class C and seismic risk category 2 for downtown Seattle, WA. These ground motions were chosen from actual earthquake events, each originating from distinct seismic sources. For instance, records from earthquakes such as the 1980 Victoria, 1989 Loma Prieta, 1994 Northridge, 1999 Chi-Chi, and 2004 Niigata events were used to simulate shallow crustal earthquakes. The 2003 Tokachi-Oki and 2011 Tohoku earthquakes were chosen to emulate interface subduction earthquakes. Furthermore, the 1992 Ferndale earthquake was included to represent intraslab motions.

Table 1: Selected ground motion subset (Note: MID = motion identification, PIA = peak input acceleration)

Target Hazard Level	Phase	MID	Earthquake	Input Direction	Achieved PIA [g]		
					X	Y	Z
43		56	1992 Ferndale, USA (Intraslab) Station: 89255	XYZ	0.06	0.07	0.10
225		59		XY	0.20	0.24	0.01
475		75	Station: 09255	XYZ	0.30	0.38	0.39
975		62	2011 Tohoku, Japan (Subduction) Station:IBRH17	XY	0.20	0.21	0.02
MCER		76		X	0.33	0.03	0.01
		82		X	0.50	0.03	0.02
		93		X	0.70	0.03	0.02
		69	2004 Niigata Chuetsu, Japan (Crustal) Station:NIG023	XYZ	0.23	0.34	0.08
		70	1999 Chi-Chi, Taiwan (Crustal) <i>Station:TCU12</i> 9	Χ	0.46	0.02	0.01
		71		Υ	0.03	0.27	0.01
<u>→ N</u>		46		XY	0.47	0.25	0.02
	Phase-1	81		XYZ	0.46	0.25	0.32
		100		XYZ	0.46	0.27	0.32
		44	1994 Northridge, USA (Crustal) Station:N Oakbank	XYZ	0.35	0.25	0.19
		77		X	0.52	0.03	0.02
		78		Υ	0.02	0.39	0.01
		79		XY	0.51	0.40	0.02
		86		XYZ	0.51	0.40	0.26
		87	1992 Ferndale, USA (Intraslab)	XYZ	0.45	0.47	0.39
		90	Station:89486	XYZ	0.64	0.64	0.68
		91	2003 Tokachi-Oki, Japan (Subduction) Station:HKD131	X	0.37	0.02	0.02
N		92	1980 Victoria, Mexico (Crustal) Station: Sahob Casa Flores	XYZ	0.47	0.51	0.30
		88	1989 Loma Prieta, USA (Crustal) Station: <i>Fremont-Emerson Court</i>	XYZ	0.53	0.72	0.18
	Payload	103	1999 Chi-Chi, Taiwan (Crustal) Station:TCU129	Υ	0.03	0.28	0.01
		110		XYZ	0.46	0.26	0.33
		105	1994 Northridge, USA (Crustal) Station:Glendora-N Oakbank	Υ	0.02	0.40	0.02

<sup>&</sup>lt;sup>1</sup> MID103, MID105, and MID110 in the payload tests were targeted to be equivalent to MID71, MID78, and MID100 in Phase-1, respectively.

To assess the specimen response under different hazard levels, the selected ground motions were amplitude-scaled to correspond to events with return periods (RP) of 43 years, 225 years, 475 years, 975 years, and the risk-targeted maximum considered earthquake, which is approximately equivalent to an event with a return period of 2475 years. For a more detailed explanation of the scaling process refer to Wichman (2023). Table 1 summarizes the sets of motions that are discussed in this paper. The RP, earthquake event, direction of input, and peak input accelerations (PIA) of the achieved motions are also summarized in Table 1.

Figure 5 displays the 5% damped acceleration spectra of the ground motions listed in Table 1. Each row in the figure represents motions at a particular hazard level, while each column represents the individual directional component (X, Y, or Z). In addition, the vibration period of the first three flexural modes of the building in each perpendicular direction, east-west (X) direction, and north-south (Y) direction are shown in dashed vertical lines. A total of 100 tests (MID1-MID100) were conducted in phase 1 of this project. Tests MID1-MID12 were conducted to tune the shake table. The data from tests MID13-MID41 was not synchronized. The modal properties in this figure on subplots of 43 y RP, 225 y RP, and 475 y RP motions are calculated from White Noise tests conducted in each of the X and Y directions before MID43 ground motion. However, the periods listed on subfigures of 975 y RP, and MCER motions are calculated from the White Noise test conducted after tests MID78 and MID88 which are the first motions in these hazard levels, respectively. Frequency Response Function (Ewins, 2000), Frequency Domain Decomposition (Brincker et al, 2001), and Stochastic State-pace Identification (Van Overschee and De Moor, 1994) methods are used to determine the building's dynamic characteristics. The vibration periods summarized in Figure 5 are the arithmetical mean of the periods predicted based on these three different identification methods as obtained using directional specific (X or Y) input White Noise mentioned above.

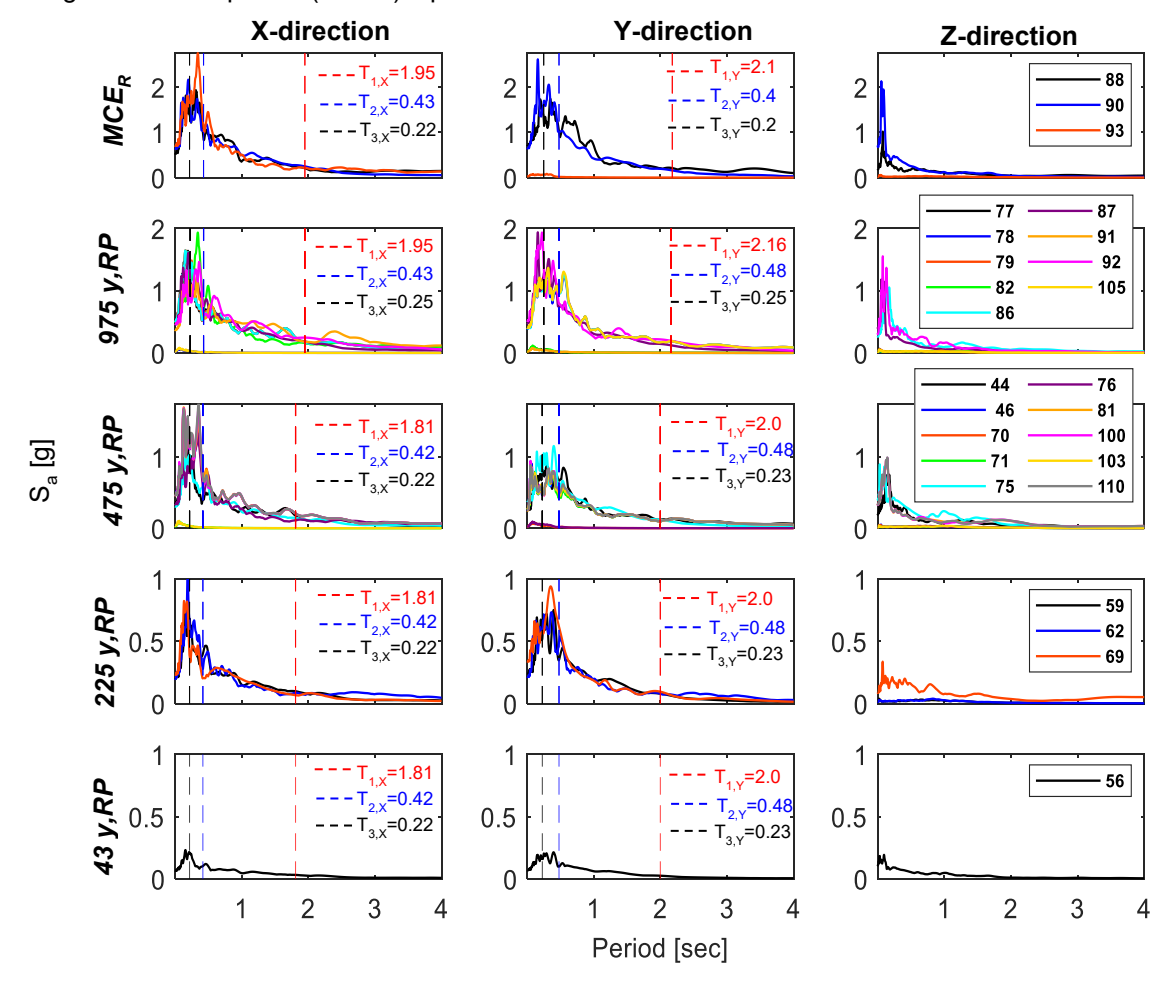


Figure 5: 5% damped elastic acceleration response spectra of selected ground motion subset

#### 3. Seismic test results

In Phase 1 and the subsequent payload phase, the stair system's performance aligned with the predictions made through numerical simulations. Notably, the stair system demonstrated robustness, and serviceable performance throughout the suite of earthquake tests, suffering no loss of function during even the largest XYZ risk-targeted maximum considered (MCE<sub>R</sub>) motions. This section summarizes preliminary findings of the earthquake tests.

## 3.1. Measured response

In Section 2.3, the diverse range of connection details integrated into the stair tower to accommodate interstory drift was discussed. To measure the displacement response of these connections, linear potentiometers and string potentiometers were utilized. This section focuses specifically on the responses of three types of connections: drift-compatible connections (DC) at levels 2.5, 3.5, 4.5, and 10.5, free connections (FC) at levels 6 and 6.5, and longitudinal slotted connections (SC) at levels 8 and 8.5. Figure 6 shows the displacement response of these connections under Loma Prieta XYZ motion scaled to MCE<sub>R</sub> target hazard level (MID88). For comparison, the interstory drifts obtained using double integration of the accelerations recorded at the stair landings are also shown. These results show that the drift-compatible connections at levels 2.5, 4.5, and 10.5 effectively accommodated the drifts in both the X and Y directions. However, at level 3.5, the drift-compatible connection didn't fully accommodate the drift due to the restraint imposed by the frame of the fire-rated shaft walls. Nevertheless, this connection's flexibility prevented damage to the stair system. On the other hand, the free connections at levels 6 and 6.5 accommodated the interstory drift sufficiently. The movement across these connections was larger than any other connection in the stair tower and in some cases, this excessive deformation resulted in damage to the handrail connections and subsequent handrail detachment. The longitudinal slotted connections at level 8 are relatively shorter than those at Level 8.5, see Figure 4b and 4d. Consequently, the slotted connection at level 8 exhibited less deformation compared to the measurement at level 8.5. It is worth noting that longitudinal slotted connections do not allow movement in the transverse direction (Y direction).

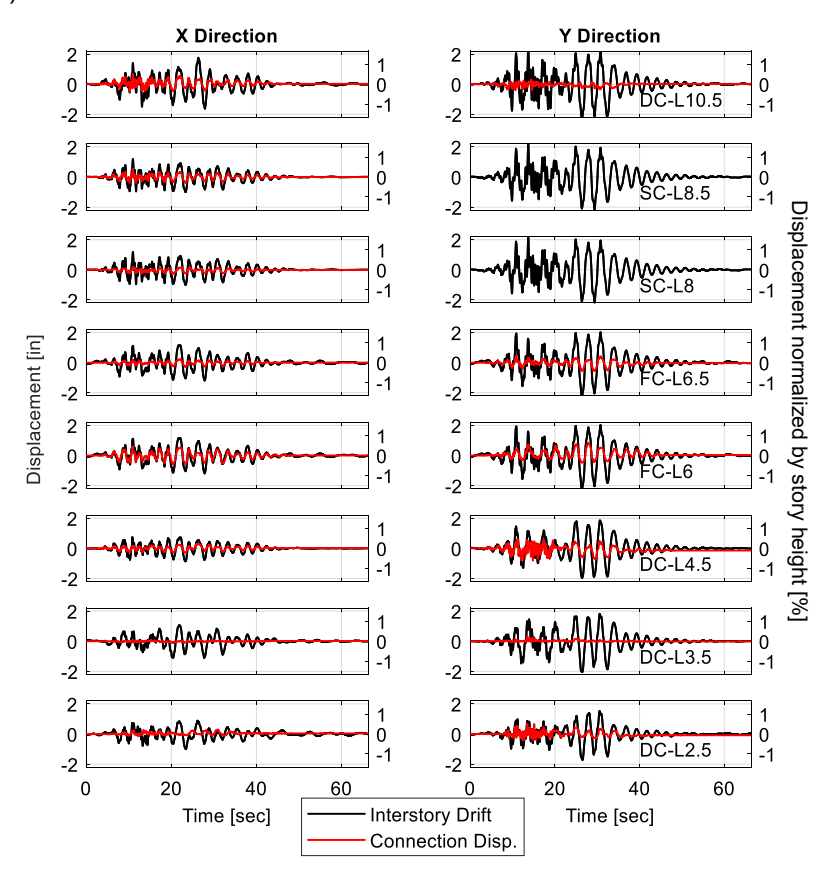


Figure-6: Displacement histories of the stair connections along with interstory drift time histories under Loma Prieta XYZ MCE<sub>R</sub> motion (MID88). DC: drift-compatible connection, FC: free connection, and SC: slotted connection

Figure 7 shows the peak connection displacement normalized by the peak interstory drift at the specific level the connection is located. Rows in the figure represent different hazard levels, and the figures are color-coded according to the MID as specified in Table 1. Different symbols are employed to distinguish between the varying components of the shake table input excitation, namely X, Y, XY, and XYZ excitation. Important observations from this figure are as follows:

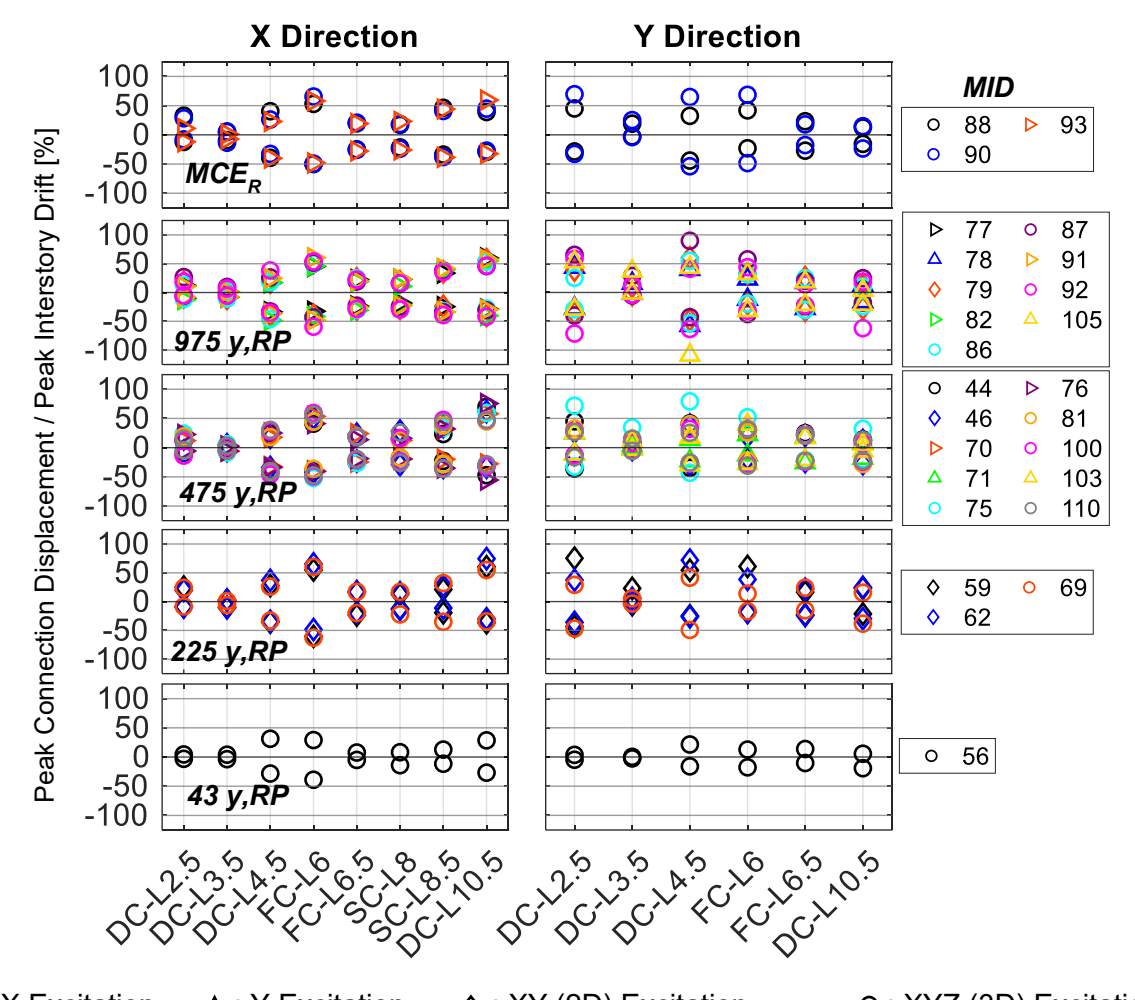
- Under motion with a 43 year return period (i.e., MID56 in Figure 7), all connections observed less than 50% of the interstory drift, however, the drift-compatible connections (DC) in particular at Levels 2.5 and 3.5 showed minimal movement (less than 10% of the interstory drift). Nevertheless, the drift-compatible connections with the dual attachment channels and those within the stair system built in traditional construction, levels 4.5 and 10.5 respectively, accommodated the drift significantly more than the DC at levels 2.5. and 3.5.
- At all hazard levels, the drift-compatible connections at level 3.5 did not effectively accommodate
  interstory drift. However, there was no significant physical damage observable at this level. This might
  be due to the flexibility in connections, and the construction slots provided. However, the construction
  slotted connections at this level were not instrumented.
- The drift-compatible connection with dual attachment channels (Level 4.5) showed superior performance in terms of accommodating drift compared to counterparts with a single attachment channel at levels 2.5 and 3.5. This is evident in the fact that this connection consistently (through all hazard levels and DOF of excitation) moved between 50% and 100% of that of the interstory drift.
- The free connection (e.g., FC at level 6) had the largest movements compared to any other connections in the stair tower. Consequently, the handrail connection at the levels with free connections observed appreciable damage due to these movements.
- The longitudinal slotted connections (SC) performed well in terms of accommodating drift. However, the slotted connections at Level 8 were shorter, resulting in more restrained and controlled displacement compared to those of Level 8.5 with longer slotted connections.
- Comparing the response of the modular stair system at Level 2 to the stair system built-in traditional construction method at Level 10, the drift-compatible connection at Level 10.5 showed a larger movement in the X direction and a smaller movement in the Y direction compared to that at Level 2.5.
- Comparing the responses of the stair system from Phase-1 to the Payload phase (e.g., MID71 to MID103, MID78 to MID105, and MID100 to MID110), despite similar input acceleration spectra (see Figure-5), the stair connection peak displacement normalized by peak interstory drift was generally larger in the Payload phase. This could be attributed to gradual bolt prestress loss and stair handrail connection damage or lower interstory drifts during the Payload phase.

#### 3.2. Physical observation

Throughout Phase-1 and the Payload phase, although the stair system remained functional, minor damage was observed in the connections of many of the handrails, particularly during the tests with larger-intensity (975-year and MCE<sub>R</sub>-scaled) motions. In addition, minor damage to the concrete stair tread, the shaft wall, and incipient connections prying were observed. This damage did not render the stair system inoperable. The former, however, indicates that there were stress points in the handrail connections that need attention and would benefit from refined design. For instance, Figure 8a shows the first detachment of handrails that occurred at Level 7.5. This was detected during inspection following a Northridge motion scaled to 975 years return period (MID79). The peak interstory drift ratio (PIDR) at level 7 during the test prior to the inspection was 1.2% in both the X- and Y-directions. Figures 8b and 8c show similar damage at levels 9 and 6, respectively. These were observed during inspection following a Tokachi motion scaled to a 975 years return period (MID91). PIDRs, in the X-direction, at levels 9 and 6 during MID91 motion were 2% and 1.9%, respectively. In addition, during the inspection after MID91, a stair handrail through thickness fracture at the critical bend region at level 8.5 was observed, see Figure 8d. Prior to observation at this level, the PIDR, in the X-direction, was 2.2%.

The fire-rated shaft walls' performance aligned with the design target. Namely, no significant damage to these walls was observed as the interior individual shaft wall units were assembled with floating gypsum board, designed to freely move with a steel channel guide. However, there were a few instances in which a gap opening between the adjacent wall panels was detected which would render reduction in the post-seismic fire rating of the shaft walls. For instance, Figure 8e documents the day light present at a gap opening at level 3

that was first observed during inspection following a Ferndale motion scaled to a 975 year return period (MID85). The final type of damage that was reported involved the prying of stringer connections (Figure 8f,g). This type of damage developed gradually, and was first observed toward the end of the Phase 1 testing.



hildrapprox : X Excitation ho : XY (2D) Excitation ho : XYZ (3D) Excitation

Figure-7: Peak connection displacement normalized by peak interstory drift. DC: drift-compatible connection, FC: free connection, and SC: slotted connection

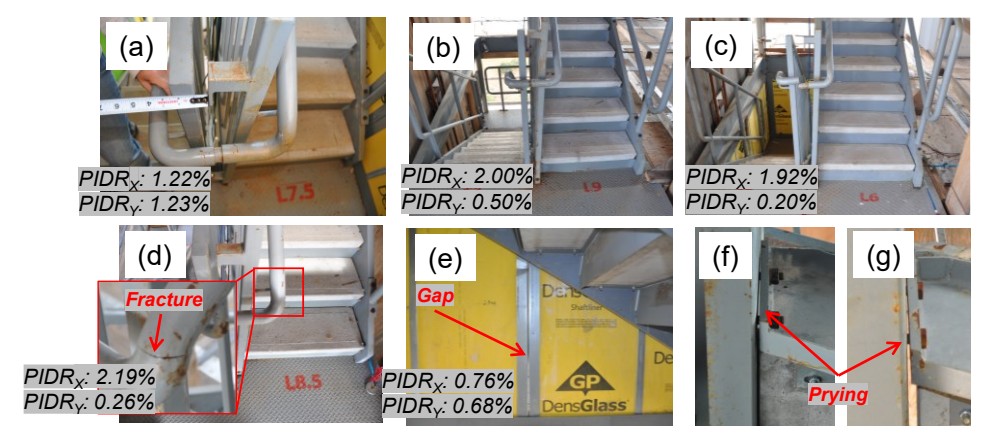


Figure-8: (a), (b) and (c) the handrail connection detachment and bolts shear off at levels 7.5, 9, and 6, respectively, (d) the handrail fracture at Level 8.5, (e) gap opening between fire-rated wall panels at level 3 (f), and (g) prying of stinger-landing channel connection at levels 10.5 and 7, respectively.

#### 4. Conclusions

In conclusion, the landmark TallWood shake table test program provided invaluable insight and information regarding the seismic performance of stair systems with seismically resilient (drift-compatible) connections. In general, the response of stair systems met the design target and accommodated the interstory drift effectively. Displacements measured at free and longitudinal slotted connections were relatively larger than those at the drift-compatible connections. Since the handrails were continuous from level 1 to the roof of the building, in select cases, particularly during motions with higher intensity (e.g., motions with 975 years RP, and MCE<sub>R</sub> hazard scaled), the handrail connection at the mid-landing and landing levels detached. This detachment of handrails was more frequently reported in the vicinity of the free and longitudinal slotted types of connections. On the other hand, the drift-compatible connection showed a superior response, compared to the free and slotted counterparts, by accommodating the interstory drifts in a more controlled manner. Observing the response of stair systems with drift-compatible connections, the stair system with a single attachment channel at Level 3 that had a fire-rated shaft wall showed the least movement across the connection. However, the flexibility of these connections still mitigated the damage, and no handrail detachment was reported in this story. In addition, more movement was observed in the drift-compatible connections with dual attachment channels compared to those with single attachment channels.

# 5. Acknowledgments

The non-structural component scope of this project is sponsored by National Science Foundation (NSF) Grant No. CMMI-1635363, US Forest Service (USFS) Grant No. 19-DG-11046000-16, Softwood Lumber Board, Computers and Structures Inc., a first-year UC San Diego graduate student fellowship (first author), and a variety of industry sponsors. The use and operation of the NHERI shake table facility are supported by NSF through Grant No.1520904. Materials and in-kind support for the stair system are provided by Construction Specialties. The overall scope of the NHERI TallWood Project is also supported under National Science Foundation (NSF) awards 1636164, 1634204, 1635156, 1634628, and the USFS Wood Innovation Fund program. Funding for the payload tests was provided by NSF under award number CMMI 2025449. The authors appreciate the aforementioned support. The opinions and findings of this study are of the authors and do not necessarily reflect those of the sponsors.

# 6. References

- Altunsu, E., Güneş, O., Öztürk, S., Sorosh, S., Sarı, A., & Beeson, S. T. (2024). Investigating the structural damage in Hatay province after Kahramanmaraş-Türkiye earthquake sequences. *Engineering Failure Analysis*, 157, 107857. doi.org/10.1016/j.engfailanal.2023.107857
- ASCE 7-16. (2017). Minimum Design Loads and Associated Criteria for Buildings and Other Structures, Standard ASCE/SEI 7-16. Structural Engineering Institute of the American Society of Civil Engineers, Reston, VA, USA. doi/book/10.1061/9780784414248
- Black, C., Aiken, A., Smith, K., Belvin, R., Peachey, A. (2017). "Seismically-Resilient Stair Systems for Buildings." *Proceedings of Structural Engineers Association of California Annual Convention (SEAOC 2017)*, San Diego, CA.
- Black, C., Aiken, I., Smith, K., Belvin, R., Peachey, A. (2020). "Shake table testing of seismically resilient stair systems for buildings." *Proceedings of the 17th World Conference on Earthquake Eng.*, Sendai, Japan.
- Brincker, R., Zhang, L., & Andersen, P. (2001). Modal Identification of Output-Only Systems Using Frequency Domain Decomposition. *Smart Materials and Structures*, 10(3), pp. 441. DOI: 10.1088/0964-1726/10/3/303.
- Bull, D.K. (2011). Stair and access ramps between floors in multi-storey building. A report at the Canterbury Earthquake Royal Commission, Christchurch, New Zealand.
- Busch, A. (2023). "Design and construction of tall mass timber buildings with resilient posttensioned mass timber rocking walls." Ph.D. thesis, Colorado School of Mines, Golden, CO.
- Dilsiz, A., Selim G., Mosalam, K., Miranda, E. Arteta, C., Sezen, H., Fischer, E., et al. 2023. StEER-EERI: 2023 Mw 7.8 Kahramanmaras, Türkiye Earthquake Sequence Joint Preliminary Virtual Reconnaissance Report (PVRR). Accessed [2023-09-26]. doi.org/10.17603/Ds2-7ry2-Gv66.

Dowden, D.M., & Tatar, A. (2024). "Shake table test of a full-scale 10-story mass timber building with uplift friction dampers." *In Proceedings of the 18th world conference on earthquake engineering, WCEE2024*, Milan, Italy.

- Ewins, D.J. (2000). *Modal Testing: Theory, Practice, and Application*. 2nd ed. Research Studies Press, England.
- Higgins, C. (2009). Prefabricated steel stair performance under combined seismic and gravity loads. *ASCE Journal of Structural Engineering*, 135(2), pp. 122-129. doi/10.1061/(ASCE)0733-9445(2009)135:2(122)
- Huang, D. (2023). "Optimized seismic design and dynamic response analysis of mass timber rocking wall lateral system." Ph.D. thesis, Colorado School of Mines, Golden, CO.
- Hutchinson, T.C., Restrepo, J.I., Conte, J., & Meacham, B. (2013). "Overview of the building nonstructural component and systems (BNCS) project." *Proceedings of ASCE 2013 Structures Congress*, Pittsburg, PA, 1485-1498. doi.org/10.1061/9780784412848.131
- Li, B., & Mosalam, K.M. (2013). Seismic performance of reinforced concrete stairways during the 2008 Wenchuan earthquake. *ASCE Journal of Performance of Constructed Facilities*, 27(6), pp. 721-730. doi.org/10.1061/(ASCE)CF.1943-5509.0000382
- Pantoli, E., Wang, X., Chen, M., Hutchinson, T.C., Meacham, B., & Park, H.J. (2013). "Shake table testing of a full-scale five-story building: performance of the major nonstructural components-egress and façades." *Proceedings of ASCE 2013 Structures Congress*, Pittsburg, PA.
- Pei, S., Lindt, J., Berman, J., Ryan, K., Dolan J.D., Pryor, S., Wichman, S., Busch, A., Zimmerman, R. (2023). Full-scale 3-D shake table test of a ten-story mass timber building. World Conference on Timber Engineering [Preprint]. doi:10.52202/069179-0276.
- Roser, William, Wichman, Sarah, Ji, Yi-En, Wynn, Sir Lathan, Ryan, Keri, Berman, Jeffrey W., Hutchinson, Tara C., and Pei, Shiling. (2022). "Evaluation of Non-structural Walls with Drift-Compatible Details in a 10-Story Mass Timber Building Shake Table Test". *ATC/SPONSE Fifth International Workshop on the Seismic Performance of Non-Structural Elements (SPONSE)* https://par.nsf.gov/biblio/10464685.
- Sorosh, S., Hutchinson, T.C., & Ryan, K.L. (2022). "NHERI TallWood 10-story Test Nonstructural, Part 4 of 4: Prefabricated Steel Stair Subassemblies." *In Proceedings of the 12th National Conference in Earthquake Engineering, Earthquake Engineering Research Institute*, Salt Lake City, UT. https://par.nsf.gov/biblio/10348730
- Sorosh, S., Hutchinson, T.C., Ryan, K.L., Wichman, S., Smith, K., Belvin, R., & Berman, J.W. (2022). "Numerical Simulation of Prefabricated Steel Stairs to be Implemented in the NHERI TallWood Building." *In Proceedings of the Fifth International Workshop on the Seismic Performance of Non-Structural Elements (SPONSE)*, Stanford, CA. https://par.nsf.gov/biblio/10464684.
- Tatar, A., & Dowden, D.M. (2022). Analytical and numerical investigation of a low-damage uplift friction damper for self-centering cross-laminated timber rocking walls. *Engineering Structures*, DOI: 10.1016/j.engstruct.2021.113836.
- Van Overschee, P., & De Moor, B. (1994). N4SID: Subspace Algorithms for the Identification of Combined Deterministic-Stochastic Systems. *Automatica*, 30(1), pp. 75-93. DOI: 10.1016/0005-1098(94)90230-5.
- Wang, X., Astroza, R., Hutchinson, T.C., Conte, J.P., Restrepo, J.I. (2015). Dynamic characteristics and seismic behavior of prefabricated steel stairs in a full-scale five-story building shake table test program. *Earthquake Engineering and Structural Dynamics*, 44(14), pp. 2507-2527. https://doi.org/10.1002/eqe.2595
- Wang, X., Ebrahimian, H., Astroza, R., Conte, J., Restrepo, J., Hutchinson, T.C. (2013). "Shake table testing of a full-scale five-story building: pre-test simulation of the test building and development of a nonstructural component and systems design criteria." *Proceedings of ASCE 2013 Structures Congress*, Pittsburg, PA.
- Wichman, Sarah (2023). "Seismic Behavior of Tall Rocking Mass Timber Walls." Ph.D. thesis, University of Washington, Seattle, Washington.
- Wynn, S., Ryan, K.L., Roser, W., Ji, Y., Sorosh, S. and Hutchinson, T., (2022). NHERI TallWood 10-story Test Nonstructural, Part 1 of 4: Project Overview and Curtain Wall Subassembly. *In 12th National Conference on Earthquake Engineering*. https://par.nsf.gov/biblio/10348727.